RUNX3 plays an important role in As_2O_3-induced apoptosis and allows cells to overcome MSC-mediated drug resistance

GUO-ZHENG PAN[1*], FENG-XIAN ZHAI[2*], YIN LU[3], ZHI-GANG FANG[3], RUI-FANG FAN[3], XIANG-FU LIU[3] and DONG-JUN LIN[3*]

[1]Renal Transplantation Center, Anhui Provincial Hospital, Hefei, Anhui 230001; [2]School of Basic Medical Sciences, Anhui Medical University, Hefei, Anhui 230032; [3]Department of Hematology, The Third Affiliated Hospital of Sun Yat-sen University, Guangzhou, Guangdong 510630, P.R. China

Received February 12, 2016; Accepted March 22, 2016

DOI: 10.3892/or.2016.5005

Abstract. The interaction between bone marrow stromal cells and leukemia cells is critical for the persistence and progression of leukemia, and this interaction may account for residual disease. However, the link between leukemia cells and their environment is still poorly understood. In our study, runt-related transcription factor 3 (RUNX3) was identified as a novel target gene affected by As_2O_3 and involved in mesenchymal stem cell (MSC)-mediated protection of leukemia cells from As_2O_3-induced apoptosis. We observed induction of RUNX3 expression and the translocation of RUNX3 into the nucleus after As_2O_3 treatment in leukemia cells. In K562 chronic myeloid leukemia cells, downregulation of endogenous RUNX3 compromised As_2O_3-induced growth inhibition, cell cycle arrest, and apoptosis. In the presence of MSC, As_2O_3-induced expression of RUNX3 was reduced significantly and this reduction was modulated by CXCL12/CXCR4 signaling. Furthermore, overexpression of RUNX3 restored, at least in part, the sensitivity of leukemic cells to As_2O_3. We conclude that RUNX3 plays an important role in As_2O_3-induced cellular responses and allows cells to overcome MSC-mediated drug resistance. Therefore, RUNX3 is a promising target for therapeutic approaches to overcome MSC-mediated drug resistance.

Correspondence to: Professor Dong-Jun Lin, Department of Hematology, The Third Affiliated Hospital of Sun Yat-sen University, 600 Tianhe Road, Guangzhou, Guangdong 510630, P.R. China
E-mail: lindongjun163@163.com

[*]Contributed equally

Abbreviations: RUNX3, runt-related transcription factor 3; MSC, mesenchymal stem cell; As_2O_3, arsenic trioxide; SDF-1, stromal cell-derived factor-1 (also known as CXCL12, C-X-C motif chemokine 12); CXCR4, C-X-C chemokine receptor type 4; APL, acute promyelocytic leukemia; ROS, reactive oxygen species; shRNAs, short hairpin RNA

Key words: runt-related transcription factor 3, mesenchymal stem cell, As_2O_3, chemokines, acute promyelocytic leukemia

Introduction

The cancer microenvironment has been implicated in playing a critical role(s) in the development of drug resistance (1). Mesenchymal stem cells (MSCs) comprise a cell type found in the cancer microenvironment (2). It has been reported that stromal cells protect tumor cells from apoptosis induced by chemotherapy either through cell-cell interactions with tumor cells or by the local release of soluble factors, such as interleukin-6, which promote survival and tumor growth (3,4). In contrast to solid tumors that invade bone marrow, leukemia originates in the marrow in close proximity to stromal cells that provide growth and survival signals (5). These signals provide the primary drug resistance mechanism in leukemia, also referred to as cell adhesion-mediated drug resistance, and may account for the minimal residual disease in tissue (6,7). We recognized the importance of MSC in drug resistance, and we propose that determining how leukemia cells communicate with the surrounding tissue will pave the way for eliminating residual leukemia cells that are 'hiding' in stromal niches.

Leukemia-stroma interactions and the consequences on tumor survival involve CXCR4/CXCL12 signaling (3). C-X-C motif chemokine 12 (CXCL12), previously called stromal cell-derived factor-1 (SDF-1), is a chemokine that is constitutively secreted by MSC and facilitates the interaction between leukemia cells and stromal cells via its cognate receptor CXCR4 (8). Intracellular CXCR4 levels are significantly elevated in B-CLL (9,10), B-cell acute lymphoblastic leukemia (11), multiple myeloma (12), some AML (13), and CML (3). The CXCR4 antagonist, AMD3100 (Plerixafor), has been in clinical trials to resensitize leukemia cells to cytotoxic drugs in co-cultures with MSC (14). However, blocking the CXCR4 only partially overcomes stromal cell-mediated drug resistance (14-17). Therefore, other interactions between leukemia cells and the tumor microenvironment may provide alternative therapeutic targets.

Arsenic trioxide (As_2O_3) is a clinically effective agent in the treatment of acute promyelocytic leukemia (APL) in primary cases (18,19), relapsed cases (20), and in ATRA-resistant patients (21). As_2O_3 has also been shown to induce apoptosis and display antiproliferative effects in Hodgkin's lymphoma,

myeloid leukemias that express BCR-ABL tyrosine kinase as well as HL-60 cell types that overexpress Bcl-2, Bcl-X (L), MPR, and MRP proteins (22-25). Low-dose As_2O_3 induces partial differentiation, while high-dose As_2O_3 triggers apoptosis (26). Degradation of PML-RARα and PML is the most important role that As_2O_3 plays in the differentiation of APL cells (27). Mitochondrial pathway is the principle mechanism of As_2O_3-induced apoptosis (28). Intracellular reactive oxygen species (ROS) also play a role in apoptosis (29). However, the molecular mechanism by which As_2O_3 modulates apoptosis remains unclear. Identification of the genes regulated by As_2O_3 will aid in developing our understanding of the mechanisms of As_2O_3 therapy for the treatment of leukemia.

A downstream target of the TGFβ tumor suppressor pathway, RUNX3, functions as a candidate tumor suppressor (30,31), RUNX3 modulates cellular proliferation and apoptosis through transcriptional regulation of genes, such as the growth regulator p21 and the pro-apoptotic gene Bim (32,33). RUNX3 is an important molecule that links the oncongenic Wnt and the tumor-suppressive TGFβ pathways in intestinal carcinogenesis (34). RUNX3 exhibits dynamic shuttling between the nuclear and cytoplasmic compartments (35), and RUNX3 is found tightly associated with components of the nuclear architecture. The targeting of RUNX3 to the nuclear matrix may have significant biological consequences and may regulate RUNX3 activity (35,36). In our study, we report that RUNX3 plays a critical role in As_2O_3-induced apoptosis and MSC-mediated drug resistance in leukemia cells.

Materials and methods

Generation of mesenchymal stem cells. Three milliliters of bone marrow cells were obtained from normal donors aged between 20 and 50 years old who had provided written consent under the Ethics Committee of Sun Yat-sen University, which approved the protocol according to the Declaration of Helsinki. To isolate MSC, bone marrow mononuclear cells were isolated via density gradient centrifugation over Percoll (Amersham Pharmacia Biotech, Little Chalfont, UK). Immediately after centrifugation, isolated mononuclear cells were resuspended at $5x10^3$ cells/cm^2 in α-modified Eagle's medium (αMEM) with high glucose concentration (Gibco, UK), 10% fetal bovine serum (FBS; Lonza, UK), and 1% penicillin-streptomycin (Gibco). Cells were cultured at 37˚C in a humidified atmosphere containing 5% carbon dioxide. After 72 h, non-adherent cells were removed. When the cells were 70-80% confluent, adherent cells were trypsinized and expanded for 3-5 weeks. Before use in experiments, the identity of MSC was verified by checking for positivity of CD105, CD106, CD73,CD90,CD144, HLA-class I, and the lack of expression of CD45, CD34, CD133.

Co-culture experiments. For co-culture experiments, mesenchymal stem cells were seeded the day before the experiment onto 6-well plates (Corning Life Sciences) at a concentrationof $1x10^5$ cells/well and incubated at 37˚C in 5% CO_2. After confirming the confluence of the stromal layer by phase contrast microscopy, K562 or NB4 cells were added onto the MSC layers separately at a ratio of 20:1. For assessment of MSC-derived drug resistance, cells were treated with As_2O_3 at the indicated time points. Next, K562 or NB4 cells were collected from the top layer leaving the adherent stromal layer intact. Then, K562 and NB4 cells were assayed for cell viability. MSC contamination, assessed by FACS as the fraction of CD19-negative cells, was always <1%. For experiments with AMD3100 and As_2O_3 treatment, K562 cells were pre-incubated for 4 h with AMD3100 and seeded onto confluent marrow stromal cell layers. After 4 h, As_2O_3 was added for a further 24 h. Then, the K562 cell layer was vigorously washed off and collected as previously described.

Cell transfection. A short hairpin RNA (shRNAs) plasmid against human RUNX3 and control shRNA were purchased from Joekai Biotechonology LLC (Shanghai, China) and transduced into cells by electroporation. Electroporation was performed with a Gene Pulser Xcell Unit (Bio-Rad Laboratories, Inc., Hercules, CA, USA) under conditions of 250 V, 1200 μF, and exponential wave. Clones were selected with G418 (500 μg/ml). The RUNX3 expression plasmid PCDNA3.1/RUNX3 was constructed using full-length RUNX3 cDNA, as described previously (37). K562 cells were transfected using Lipofectamine LTX from Invitrogen. Empty vectors were transfected as controls.

Cell cycle analysis. K562 cells expressing scrambled or RUNX3-targeting shRNA were incubated with As_2O_3. After incubation, the cells were harvested and resuspended in 500 μl of cold PBS and cold ethanol (1.5 ml) for 2 h at 4˚C, followed by incubation with 0.1% sodium citrate containing propidium iodide (PI) 0.05 mg and 50 μg RNase for 30 min. Finally, the cell cycle analysis was detected by flow cytometry (FC500; Beckman Coulter, Miami, FL, USA), and the proportion of cells within the G0/G1, S, and G2/M phases of the cell cycle were analyzed using the MultiCycle AV DNA Analysis software (Phoenix Flow Systems).

Quantitative reverse transcriptase-polymerase chain reaction. Total RNA was extracted from each sample using the Total RNA Extraction kit (Invitrogen), following the manufacturer's instructions. The concentration of RNA was measured by spectrophotometry. Total RNA was reverse transcribed to cDNA with reverse transcriptase reagents (Takara, Nanjing, China), according to the manufacturer's protocol. Specific primers for RUNX3 and GAPDH genes were designed based on sequence data from the GenBank database. The primers were purchased from Invitrogen Biological Engineering Technology & Services Co., Ltd. For human RUNX3 transcripts, 5'-AGGCATTGCGCAGCTCAGCGGAGTA-3' was used as a sense primer and 5'-TCTGCTCCGTGCTGCCCT CGCACTG-3' as an antisense primer. For the human GAPDH transcripts, 5'-TCACAGGGGTTCCCTTCTCTC-3' was used as a sense primer and 5'-CACTTCTTTGTGCCATCCATGG-3' as an antisense primer. Conditions for all PCRs were optimised on an iCycler iQ (Bio-Rad Laboratories, Inc.), and the optimum annealing temperature was 60˚C.

Immunofluorescence microscopy. Cells were incubated on poly-L-lysine-coated slides for 30 min, washed gently with PBS and fixed in 10% methanol at room temperature. After washing with PBS, the cells were permeabilized with 0.1% Triton in PBS

for 60 min at room temperature. The cells were then incubated with the rabbit anti-RUNX3 antibodies (BD Biosciences) overnight at 4°C. After washing with PBS, the slides were incubated with the secondary antibody, Alexa 555-conjugated goat anti-rabbit immunoglobulin G (IgG; Molecular Probes), for 2 h and then washed with PBS. Nuclei were stained with 10 nM DAPI, and cells were then subjected to fluorescence microscopy.

Morphological detection of apoptosis. Morphological evaluation of apoptotic cell death was performed using the Hoechst 33258 kit (KeyGen Biotech), according to the manufacturer's instructions. Cells were cytospun, stained with Hoechst 33258, and observed with light microscopy.

CXCL12 enzyme-linked immunosorbent assay. After culturing mesenchymal stem cells in 24-well plates for 24 h, medium was collected and concentrated by ultrafiltration. CXCL12 levels in the medium were assayed with a Human CXCL12/SDF-1 α immunoassay kit (R&D Systems, Abingdon, UK) according to the manufacturer's instructions. Samples were run in triplicate.

Flow cytometry analysis of CXCR4 expression. Monoclonal antibodies against human CXCR4-PE (BD Pharmingen, DakoCytomation) were used for flow cytometry analysis. PE-conjugated IgG1 and IgG2a control monoclonal antibodies were from Cell Signaling Technology, Inc.

Transmigration assays. For quantitative transmigration assays, K562 cells ($5x10^4$ cells) were placed in the upper chamber of a Transwell system (24-well plate, 5 μM-pore filter; Corning Life Sciences) in a total volume of 150 μl DMEM medium. Next, 600 ml of the supernatant was concentrated 10-fold, and placed in the lower chamber of the Transwell. Further control wells assessed the chemotactic activity of recombinant CXCL12 (rCXCL12) at concentrations of 100 ng/ml. Cells were harvested from the lower chamber after 3 h and counted using a hemocytometer.

Annexin V staining. Apoptosis was measured using the Calbiochem assay kit (Calbiochem, San Diego, CA, USA) according to the manufacturer's instructions. K562 cells expressing scrambled or RUNX3-targeting shRNA were incubated with As_2O_3. After incubation, cells were washed with phosphate-buffered saline (PBS) and stained using phycoerythrin-labeled Annexin V. Numbers of both RFP- and Annexin V-positive cells were determined by flow cytometry. In some cases, the Annexin V-propidium iodide staining kit (Calbiochem) was used instead, according to the manufacturer's protocol.

Western blot analysis. Cells were cultured with the indicated concentrations of As_2O_3 for the specified times, harvested, washed, and lysed using RIPA buffer containing protease inhibitors. After normalization for total protein content (60 μg/lane), the samples were subjected to 12% SDS-PAGE and then transferred to a PVDF membrane. After blocking with 5% non-fat dry milk and 0.1% Tween-20 in Tris-buffered saline, the membranes were incubated with the following primary antibodies: Mcl-1 (Cell Signaling Technology, Inc.), RUNX3 (BD Pharmingen), p21, Bax, Bcl-2, cleaved caspase-3, cleaved caspase-9, and β-actin (all from Cell Signaling Technology, Inc.). After extensive rinsing with TBST, the membranes were incubated with HRP-conjugated anti-mouse or rabbit secondary antibodies (Cell Signaling Technology, Inc.), and proteins were detected with the use of an enhanced chemiluminescence system (EMD Millipore, Billerica, MA, USA) and captured on a light-sensitive imaging film.

Statistical analysis. All experiments were repeated in triplicate. The data are reported as the mean ± SEM. Statistical analyses were performed using Student's t-test or one-way ANOVA. Probability (P) value of 0.05 was considered to be significant (SPSS v13.0 for windows).

Results

As_2O_3 induces expression of RUNX3 and translocation of RUNX3 into the nucleus. To determine whether the expression of RUNX3 is induced by As_2O_3 treatment, western blot analysis was performed to detect the level of total RUNX3 and the RUNX3 target gene, p21. As shown in (Fig. 1A), As_2O_3 treatment resulted in the elevation of total RUNX3 in K562 and NB4 cells in a dose-dependent manner. Elevation of RUNX3 levels was observed at 3 h post-treatment with 5 μM As_2O_3 in NB4 cells, and expression levels reached a peak at 9 h post-treatment. An increase in RUNX3 expression was detected at 1 h following treatment with 3 μM As_2O_3 in K562 cells, and expression levels reached a peak at 4 h post-treatment (Fig. 1B). Similarly, we also observed that the expression of RUNX3 mRNA was enhanced after As_2O_3 treatment in both K562 and NB4 cell lines. Protein levels of p21 were elevated in a dose- and time-dependent manner and corresponded to the elevation of RUNX3 observed following As_2O_3 treatment. Immunofluorescence staining revealed that RUNX3 was located mainly in the cytoplasm before As_2O_3 treatment and accumulated in the nucleus following As_2O_3 treatment (Fig. 1C). Consistent with the results obtained using NB4 cells, our analysis of K562 cells and primary APL blast cells from three patients revealed that RUNX3 localized in the cytoplasm prior to As_2O_3 treatment and translocated into the nucleus following As_2O_3 treatment. It has been previously reported that As_2O_3 treatment resulted in elevation in cellular ROS stores and production. In our studies, treatment of cells with As_2O_3 also resulted in the generation of ROS (Fig. 1D). This ROS induction seems to be necessary for As_2O_3-dependent elevation of RUNX3 because pre-treatment of cells with NAC, a scavenger of ROS, resulted in the inhibition of As_2O_3-induced expression of RUNX3 (Fig. 1E).

RUNX3 is required for As_2O_3-induced apoptosis. We next determined the role of RUNX3 in As_2O_3-induced apoptosis using RNA interference to reduce RUNX3 mRNA. We established two stable clones expressing shRNA specific to RUNX3, designated A2 and B4, and a scramble shRNA-expressing clone, designated SCR. Western blot analysis with anti-RUNX3 antibody revealed that endogenous RUNX3 protein levels were markedly diminished in A2

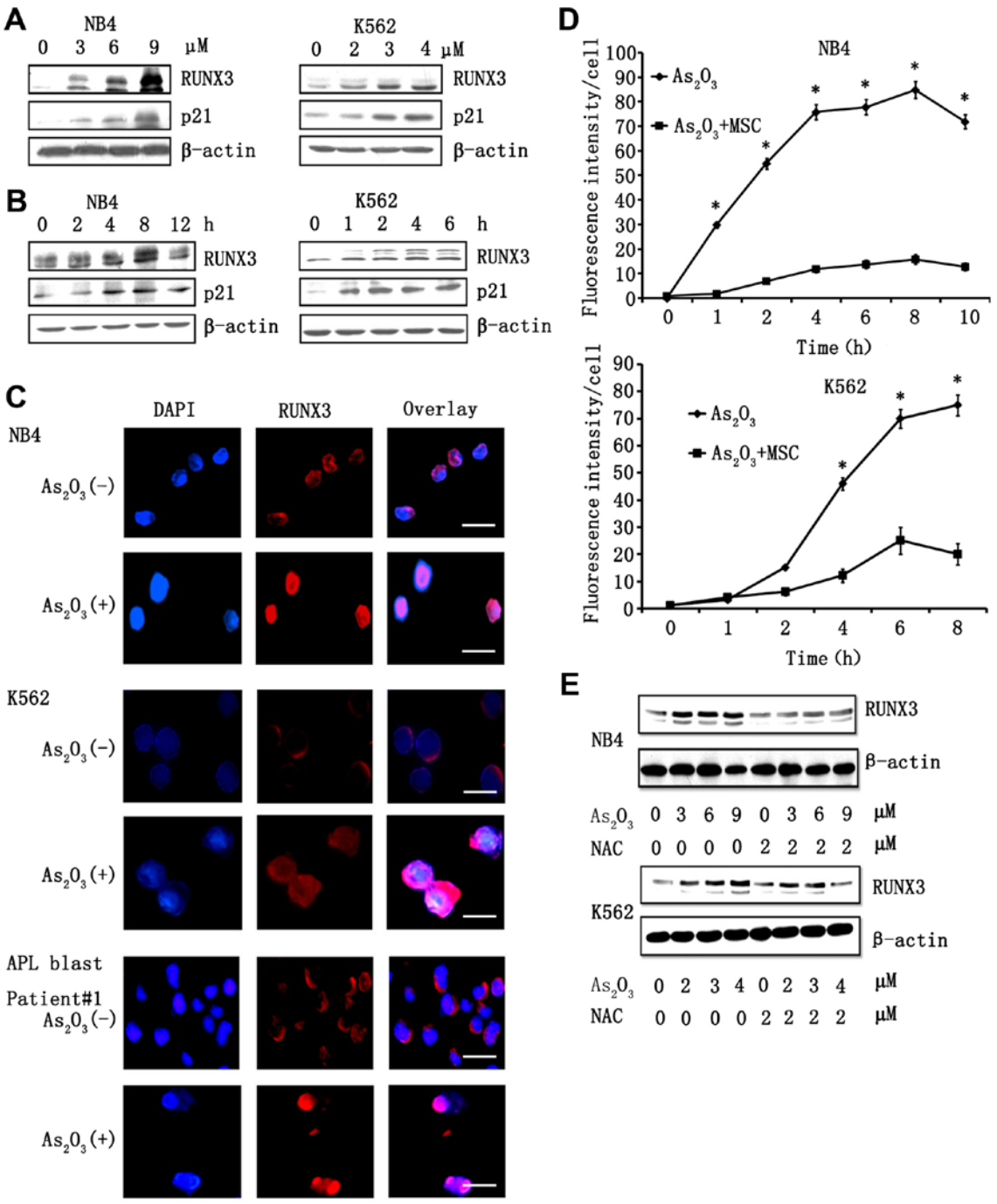

Figure 1. As_2O_3 induces expression of RUNX3 and translocation of RUNX3 into the nucleus. (A) NB4 or K562 cells were incubated with different concentrations of As_2O_3 for the indicated periods. Total protein was extracted and analyzed by western blot analysis with antibodies against the indicated antigens. β-actin was used as an internal control. (B) NB4 cells, K562 cells or primary APL blast cells were incubated with 6 or 3 μM As_2O_3 for 12 h. After fixation and permeabilization, cells were incubated with anti-RUNX3 antibody and Alexa 555-conjugated goat anti-rabbit IgG (red). The nuclei were stained with DAPI (blue), and cells were subjected to fluorescence microscopy. Scale bar, 20 μm. (C) NB4 or K562 cells were pre-incubated with As_2O_3 (6 or 3 μM) for the indicated time with or without MSC. Cells were then analyzed by flow cytometry for the presence of ROS as described in Materials and methods. Data are expressed as the fold increase in mean fluorescence over untreated samples and represent the mean ± SD of three independent experiments. $^*P<0.05$ compared with K562 incubated with MSC. (D) Pre-treatment of cells with *N*-acetylcysteine (5 mM, 30 min) attenuated the expression of RUNX3 in NB4 or K562 cells. (E) The expression of RUNX3 was analyzed by western blot analysis in cells treated with As_2O_3 for the indicated times.

clones and significantly reduced in the B4 clone compared with SCR (Fig. 2A). Cell growth assays showed that A2 cells exhibited significantly enhanced growth compared with SCR cells. As_2O_3 inhibited the growth of SCR cells, but this growth inhibition was compromised in the RUNX3 shRNA-transduced cells treated with As_2O_3 (Fig. 2B). Next, we examined the involvement of RUNX3 in As_2O_3-induced apoptosis and cell cycle arrest. As shown in (Fig. 3A), the ratio of Annexin V and propidium iodide-positive cells was increased in a time-dependent manner, and 21.6% of the SCR cells were positive on the second day after As_2O_3 treatment. By contrast, apoptosis was significantly reduced during

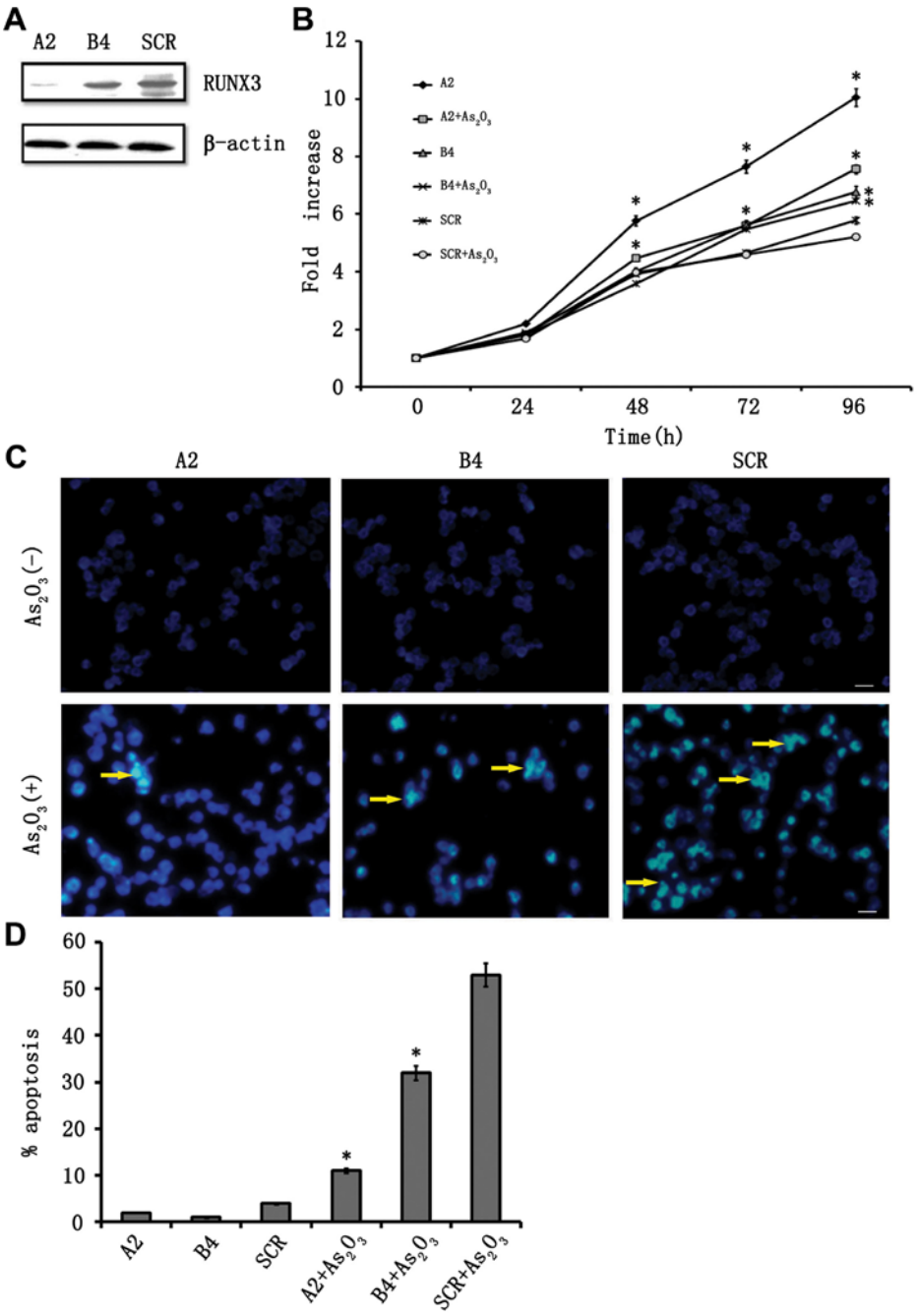

Figure 2. Knockdown of RUNX3 suppresses As_2O_3-induced cell cycle arrest and apoptosis in K562 cells. (A) Total protein was extracted from SCR or RUNX3 shRNA expressing cells and subjected to western blot analysis with antibodies against the indicated antigens. β-actin was used as an internal control. (B) SCR or RUNX3 shRNA expressing cells were incubated with 3 μM As_2O_3 for the indicated time periods. Cell growth was assessed by the Cell Counting kit-8. The results are presented as the mean ± SE of three independent experiments relative to the results obtained at day 0. $^*P<0.05$ compared with SCR treated with As_2O_3. (C and D) Morphologic changes were examined by Hoechst 33258 staining and fluorescence microscopy. $^*P<0.05$; Scale bar, 50 μm.

the observation periods up to day 2 in RUNX3 knockdown clones (Fig. 3A and B). Similar results were obtained from our Hoechst 33258 staining analysis (Fig. 2C and D). Fig. 6H shows that re-expression of RUNX3 enhanced sensitivity of K562 cells to As_2O_3 in a dose-dependent manner. Transduction of control constructs alone did not alter cellular response to As_2O_3. The percentages of cells in G1, S, and G2/M phase are illustrated in Fig. 3C and D. In SCR cells, treatment with As_2O_3 increased the fraction of cells in G2/M progressively from 8.95 to 27.61%. However, suppression of RUNX3 expression by RUNX3 shRNA attenuated As_2O_3-induced cell cycle arrest. Consistent with these results, p21 expression was suppressed in the A2 and B4 clones after As_2O_3 treatment. A decrease in the Mcl-1 protein was observed after treatment with As_2O_3 in SCR clones, though this reduction in Mcl-1 levels was compromised in A2 and B4 clones (Fig. 3E).

Mesenchymal stromal stem cells protect leukemia cells from As_2O_3-induced apoptosis. To assess whether MSC could protect leukemia cells from As_2O_3-induced apoptosis, K562 and NB4 cells were exposed to a range of As_2O_3 concentrations in the presence or absence of MSC. After 24 and 48 h,

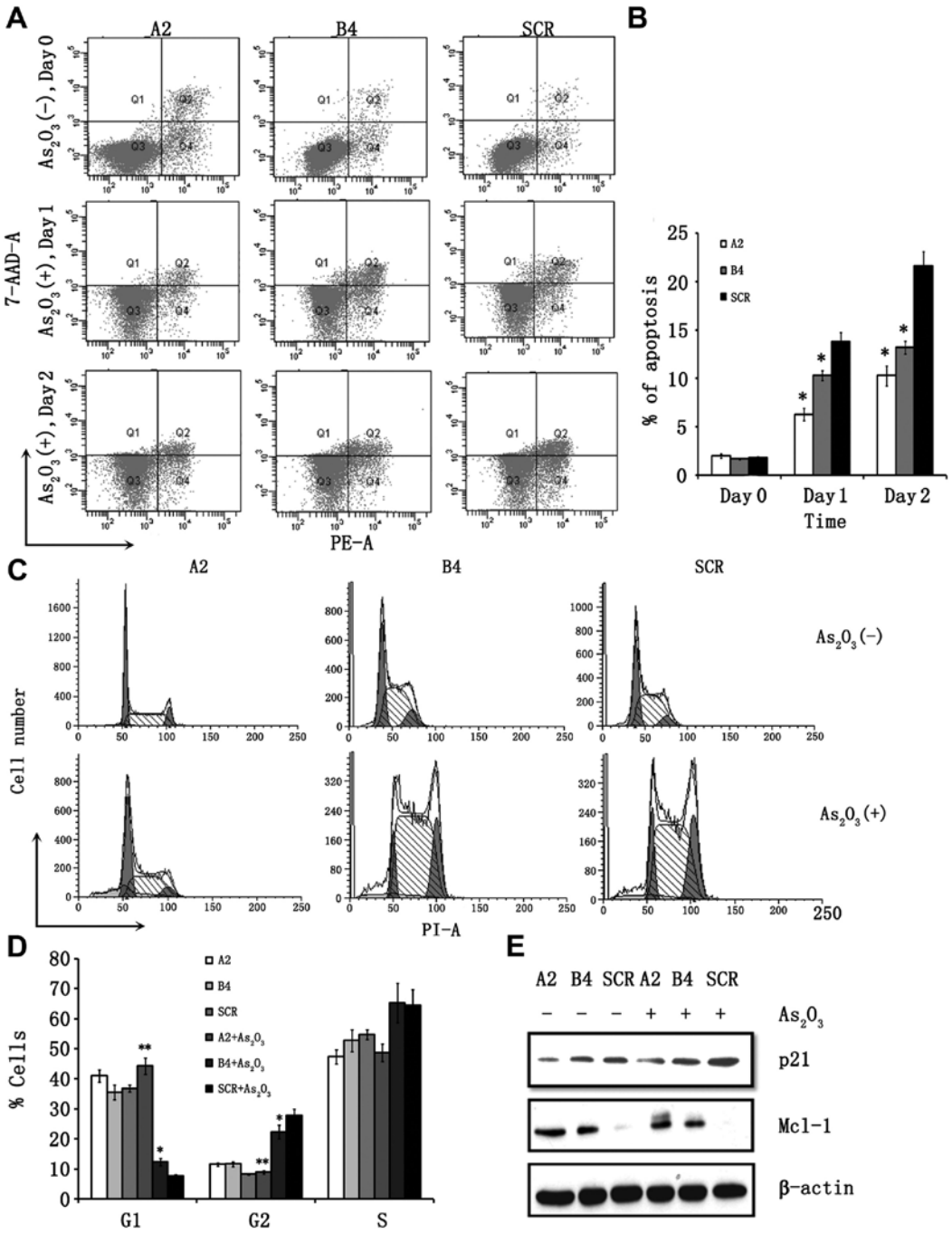

Figure 3. (A and B) Annexin V-positive cells were detected by FACS analysis. The results are presented as the mean ± SE of three independent experiments. *P<0.05 compared with SCR. (C and D) Cell cycle arrest was determined by propidium iodide staining and FACS analysis. *P<0.05, **P<0.01 compared with SCR. (E) SCR or RUNX3 shRNA expressing cells were incubated with 3 μM As_2O_3 for 12 h. Total protein was extracted and analyzed by western blot analysis with antibodies against the indicated antigens. β-actin was used as an internal control.

cells were analyzed by probing for Annexin V and propidium iodide (Fig. 4A). While exposure of NB4 cells to As_2O_3 for 24 or 48 h in control cultures induced apoptosis in a dose-dependent fashion (6.5±2, 9.2±3.5 and 13.5±3.7% of Annexin V/propidium iodide$^+$ cells for 24 h; 8±2.8, 15.9±4.1 and 38.1±5.4% for 48 h for As_2O_3 at 3, 6 and 9 μM, respectively), the proportion of apoptotic NB4 cells in the presence of MSC was significantly reduced (6.7±1.8, 7.1±3 and 8.1±2.6% for 24 h; 7.7±3.3, 8.4±3.5 and 16±4.2% for 48 h, with As_2O_3 at 3, 6 and 9 μM, respectively; P=0.003, 0.015 and 0.024, NB4 vs. NB4 + MSC with 3, 6 and 9 μM As_2O_3, respectively) (Fig. 4A). As shown in Fig. 4A, the protective effect of MSC was also observed for K562 cells. No significant protection was observed when CML cells were cultured and treated on a monolayer of endothelial cells.

We also determined whether MSC affect As_2O_3-induced cell cycle arrest. As shown in (Fig. 4B and C), As_2O_3 treatment of K562 cells resulted in a dose-dependent accumulation of cells with 4N and <2N sub-G1 DNA content, which suggests induction of G2/M-phase cell cycle arrest and apoptosis. MSC robustly reduced the proportion of G2/M-phase and sub-G1 cells. MSC did not significantly affect cell cycle arrest induced

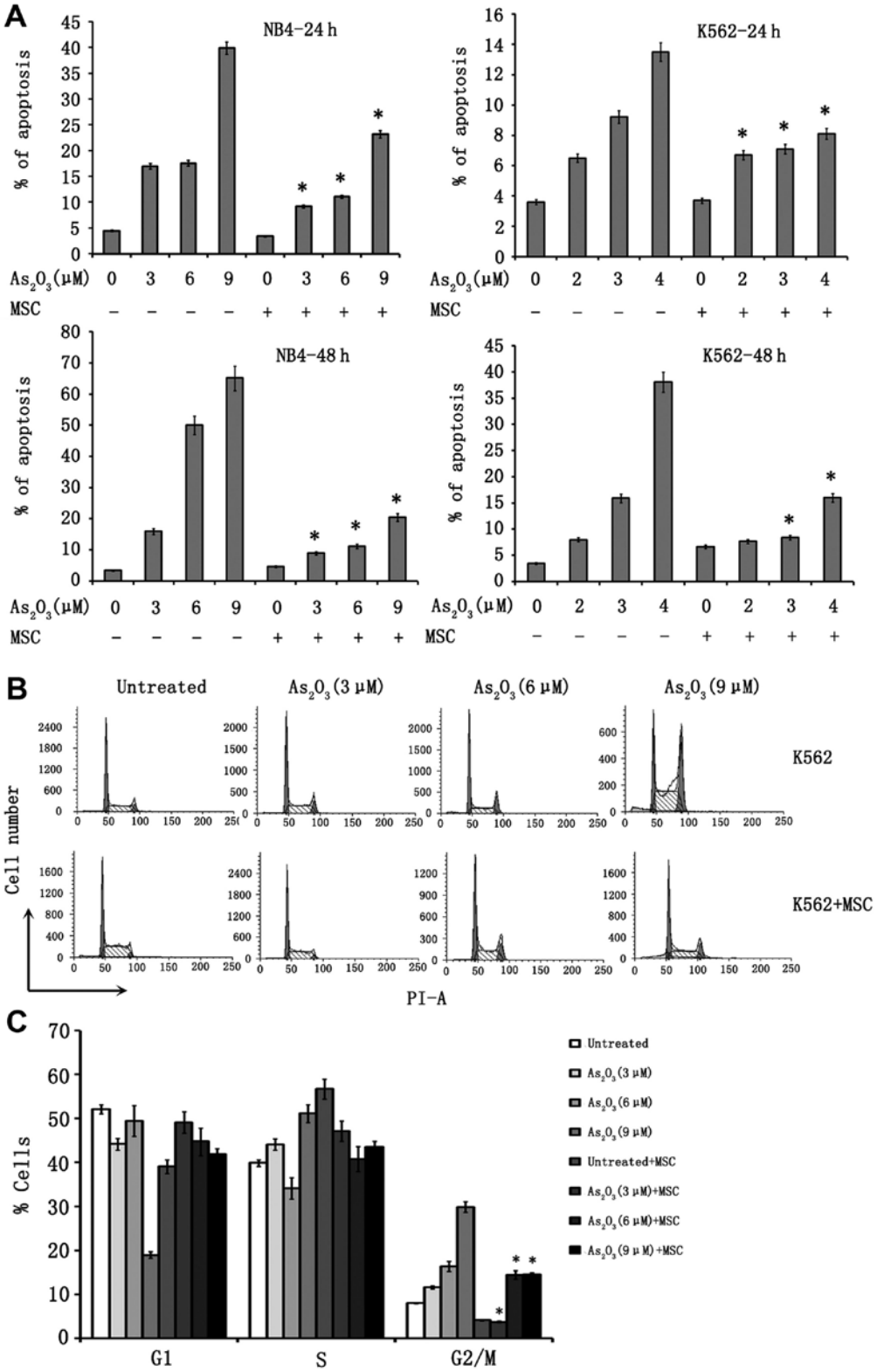

Figure 4. Mesenchymal stromal stem cells reduce As_2O_3-induced responses. (A) K562 or NB4 cells were cultured alone or in the presence of MSC. After 24 h, cells were treated with As_2O_3 at various concentrations and apoptosis was quantified after a further 24 or 48 h by Annexin V and propidium iodide staining. *P<0.05 compared with K562 incubated without MSC. (B and C) Cell cycle progression was measured by propidium iodide staining.

by As_2O_3 in NB4 cells. To determine if MSC modulate the level of ROS, K562 and NB4 cells incubated with or without As_2O_3, either in the presence or absence of MSC, were analyzed for ROS by DCFDA staining. As shown in Fig. 1D, the level of ROS in NB4 cells increased after treatment with 6 μM As_2O_3 in a time-dependent manner; however, MSC were able to attenuate the quantity of ROS produced following As_2O_3 treatment.

The intrinsic, mitochondrial pathway is the principal mechanism of As_2O_3-induced apoptosis. In the mitochondrial

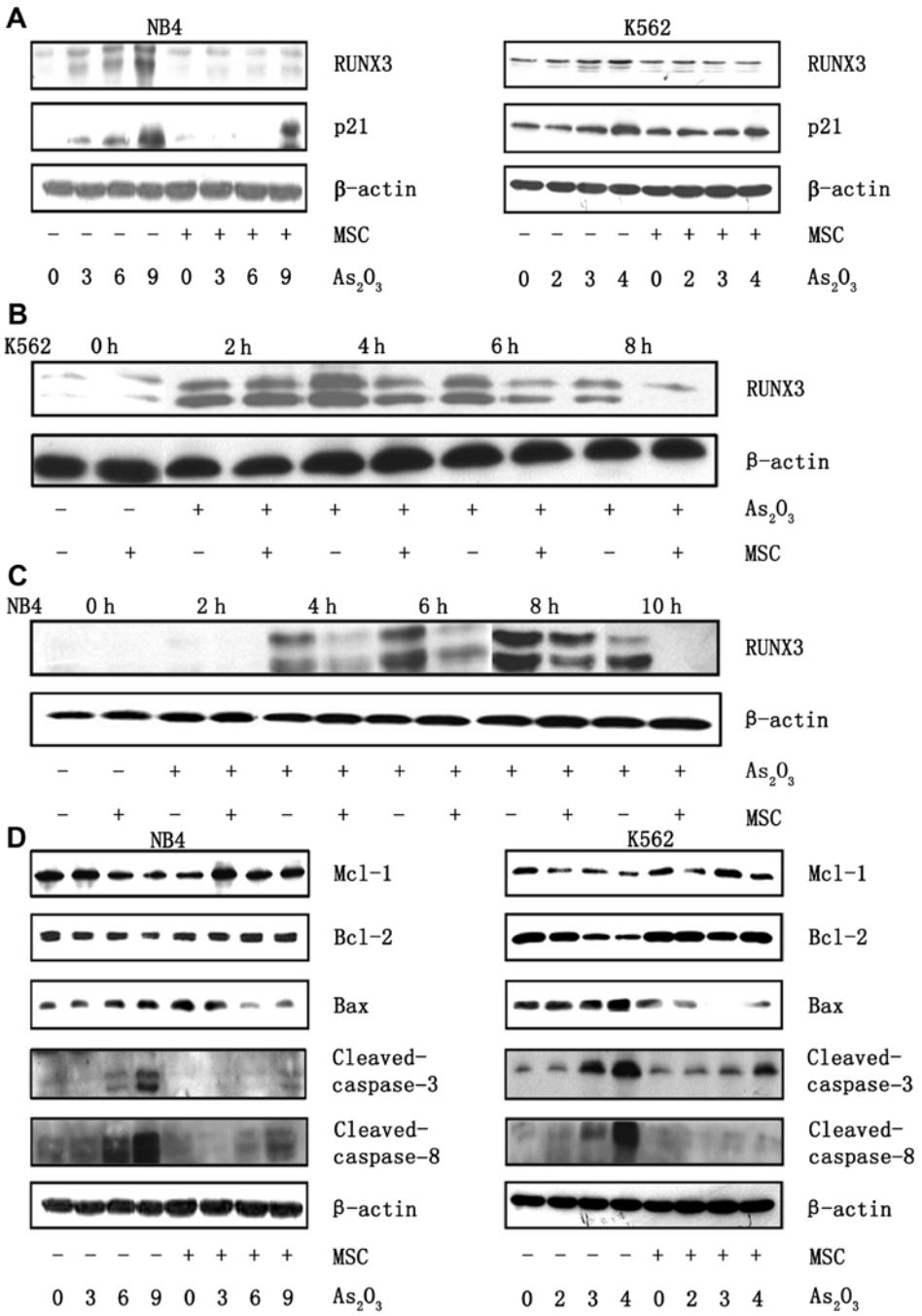

Figure 5. MSC reduce the expression of RUNX3 induced by As_2O_3. (A) K562 or NB4 cells were cultured alone or in the presence of MSC. After 24 h, cells were treated with As_2O_3 at various concentrations. Total protein was extracted 24 h post-treatment and analyzed by western blot analysis with antibodies against the indicated antigens with RUNX3 and p21. β-actin was used as an internal control. (B and C) Nuclear extract from K562 or NB4 cells was prepared at the indicated time points and subjected to western blot analysis. (D) Total protein was extracted and analyzed by western blot analysis with antibodies against the indicated antigens. β-actin was used as an internal control.

apoptotic pathway, the ratio of expression of pro-apoptotic Bax to that of anti-apoptotic Bcl-2 ultimately results in either cell death or survival. We determined the effect of MSC on the Bax/Bcl-2 ratio. Upregulation of Bax expression, as well as downregulation of Bcl-2 expression induced by As_2O_3, was blocked in the presence of MSC (Fig. 5D).

MSCs have been found to protect NB4 and K562 cells from As_2O_3-induced apoptosis, and this protection mechanism is related to the expression of apoptotic proteins. We measured protein levels of cleaved caspase-3 and cleaved caspase-8. Consistent with the previous report, As_2O_3 treatment induced the activation of caspase-8, whereas this modulation was not noted in the presence of MSC. As_2O_3-induced death of cells is associated with strong activation of caspase-3, which was significantly inhibited when cells were treated in the presence of MSC (Fig. 5D). Additionally, there were low levels of Mcl-1 protein in NB4 and K562 cells treated with As_2O_3. However, in the presence of MSC, the decrease in Mcl-1 levels was compromised (Fig. 5D).

MSC reduce the expression of RUNX3 induced by As_2O_3 via CXCL12/CXCR4 signaling. We have demonstrated that

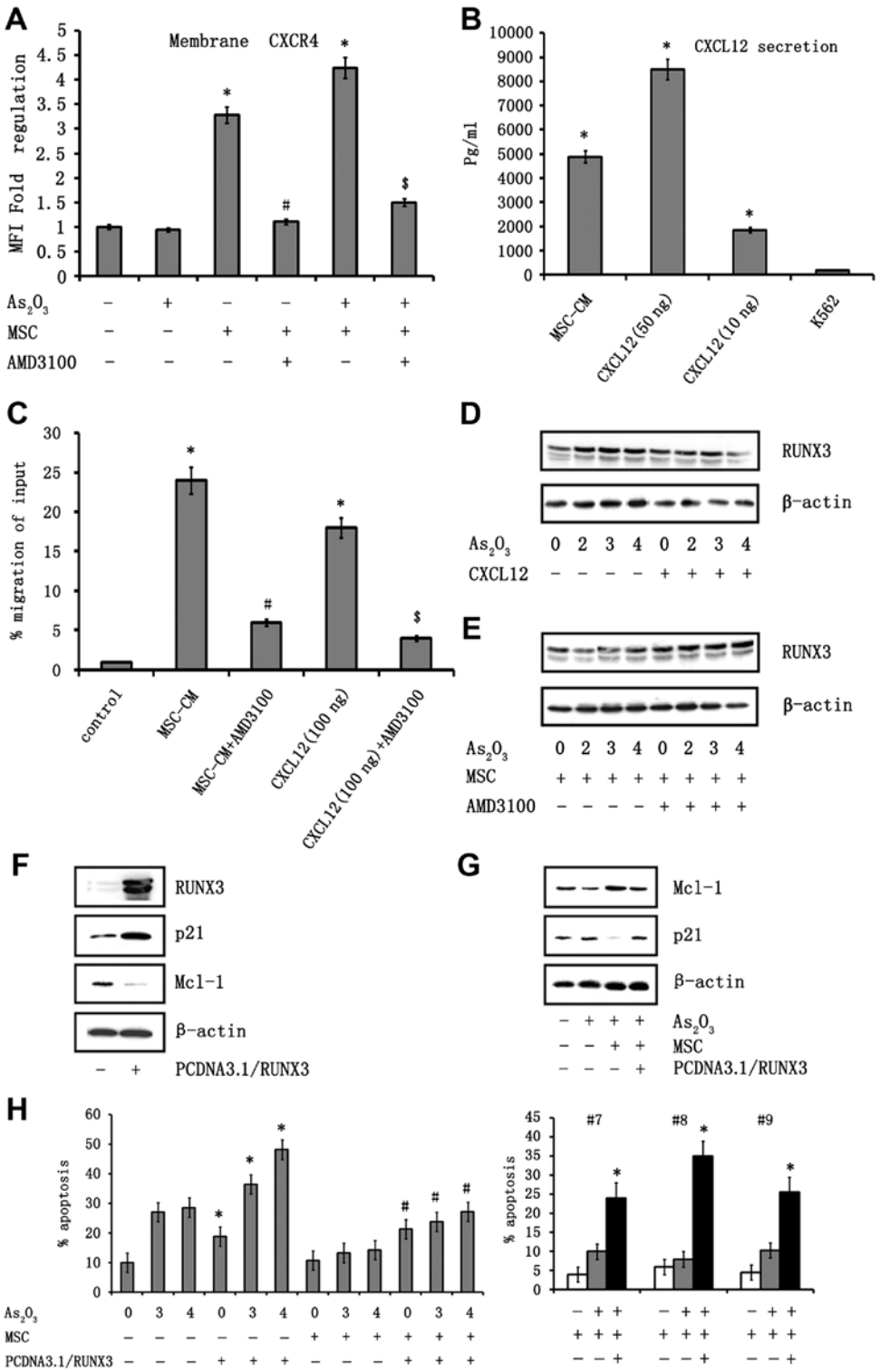

Figure 6. The expression of transcription factor RUNX3 was modulated via CXCL12/CXCR4 signaling and restore the sensitivity of K562 cells to As_2O_3. (A) K562 cells were cultured with MSC and treated with AMD3100 (50 μM), As_2O_3 (5 μM), or a combination of both. The expression level of CXCR4 compared with non-treated cells was analyzed by flow cytometry. *P<0.05 compared with non-treated cells. $^\#$P<0.05 compared with cells not treated with AMD3100. $^\$$P<0.05 compared with cells treated with As_2O_3 without AMD3100. (B) Levels of CXCL12 produced by mesenchymal stem cells from patients were detected by ELISA. The results are presented as the mean ± SE of three independent experiments. *P<0.05 compared with non-treated cells. (C) K562 cells were pre-incubated for 4 h with or without AMD3100 before being assayed for chemotaxis toward supernatant collected from MSC culture or toward rCXCL12 in a Transwell system. *P<0.05 compared with non-treated cells. $^\#$P<0.05 compared with cells not treated with AMD3100. $^\$$P<0.05 compared with cells treated with CXCL12 without AMD3100. (D) K562 cells were treated with As_2O_3 both in the absence and in the presence of CXCL12 (100 ng/ml) for the indicated times. The expression of RUNX3 was analyzed by western blot analysis. (E) K562 cells were cultured with MSC and treated with AMD3100 (50 μg/ml) or left untreated. Subsequently, cells were treated with As_2O_3 (3 μM) as indicated. Western blot analysis of total lysates from cells cultured for 10 h was performed. A representative experiment is shown. (F) Total protein was collected from vector control (VCont) and PCDNA3.1/RUNX3 expressing cells and subjected to western blot analysis with antibodies against RUNX3 and β-actin. (G) Total protein was extracted and analyzed by western blot analysis with antibodies against the indicated antigens. β-actin was used as an internal control. (H) Cells were cultured alone or in the presence of MSC. After 24 h, cells were treated with As_2O_3 at various concentrations, and Annexin V and PI-positive cells were detected by FACS 24 h post-treatment. Average histograms from three individual experiments are shown. *P<0.05 compared with non-treated cells.

RUNX3 is required for As_2O_3-induced apoptosis. To determine whether MSC modulate the expression of RUNX3, western blot analysis was used to detect the level of total RUNX3 in K562 and NB4 cells treated with As_2O_3 in the presence or absence of MSC (Fig. 5A). The presence of MSC reduced RUNX3 protein expression of cells treated with different concentrations of As_2O_3 compared to the cultures in which the leukemic cells were exposed to As_2O_3 without MSC. The expression of p21 induced by As_2O_3 was also inhibited in the presence of MSC. We next studied the subcellular distribution of RUNX3 by performing a western blot analysis on nuclear extracts from NB4 and K562 cells treated with As_2O_3 for different time intervals in the presence or in the absence of MSC. In K562 cells, the expression of RUNX3 was induced in 2 h, peaking at 4 h. In NB4 cells, RUNX3 expression was induced later and peaked at 9 h. In the presence of MSC, the level of RUNX3 in the nuclear fraction was significantly reduced at the indicated time in NB4 and K562 cells (Fig. 5B and C).

CXCL12/CXCR4 signaling is an important mediator for leukemia-stroma interaction, and this interaction has consequences on tumor survival. Therefore, we determined whether CXCL12/CXCR4 modulates the expression of transcription factor RUNX3 in K562 cells. The expression level of CXCR4 was analyzed in K562 cells by flow cytometry (Fig. 6A). K562 cells showed higher expression of CXCR4 when co-cultured with MSC. Furthermore, this increase in CXCR4 expression was enhanced in the presence of As_2O_3. The expression of CXCR4 peaked 10 min post-treatment with As_2O_3 when K562 cells were co-cultured with MSC. Second, the production of CXCL12 by MSC was analyzed in MSC supernatants by western blot analysis (Fig. 6B). To determine whether the CXCL12/CXCR4 interaction had functional activity, we investigated the chemotactic properties of MSC on K562 cells in a transmigration assay. The K562 cells migrated toward a CXCL12 gradient, demonstrating that CXCR4 was fully functional. As shown in Fig. 6C, MSC supernatant exhibited potent chemoattractive activity on K562 cells, as 24±3.2% of K562 cells migrated toward undiluted supernatant compared to 0.95±0.06% of cells that migrated in the presence of media (P=0.013). Blocking CXCR4 led to a significant reduction in chemoattractive activity in response to MSC, as well as the chemokine CXCL12 (P=0.014; Fig. 6C). All of these data indicate the presence of a functional CXCR4/CXCL12 signaling between CML cells and MSC and that this signaling is important for promoting migration.

To assess whether CXCR4/CXCL12 could modulate the expression of RUNX3, the expression of RUNX3 was analyzed in the presence of CXCL12 by western blot analysis. As shown in Fig. 6D, CXCL12 induced a significant reduction of RUNX3 mRNA expression in K562 cells. Remarkably, treatment of K562 cells with the CXCR4 antagonist AMD3100 induced RUNX3 expression (Fig. 6E). Moreover, the expression of RUNX3 was upregulated after treatment with AMD3100 in the presence of MSC, indicating that the inhibition of CXCR4/CXCL12 signaling was rescuing the expression of RUNX3.

Expression of RUNX3 overcomes MSC-mediated As_2O_3 resistance. Mesenchymal stromal cells have been found to protect leukemia cells from As_2O_3-induced apoptosis. We tested the hypothesis that the overexpression of RUNX3 could restore the effect of As_2O_3 on K562 cells. K562 cells were transfected with a RUNX3 expression vector or an empty control vector. The expression of RUNX3 in these cells was confirmed by western blot analysis (Fig. 6F). When K562 cells transfected with RUNX3 were co-cultured with MSC, the Annexin V and PI-positive cells treated with increasing concentrations of As_2O_3 was significantly increased compared to the cultures in which leukemic cells transfected with empty vector were exposed to As_2O_3 in the presence of MSC. Similar results were observed from APL primary blast patients (Fig. 6H). In addition, we found that p21 protein expression was significantly increased after exposure to As_2O_3 in cells transfected with the RUNX3 expression vector in the presence of MSC, but not for cells transfected with control vector (Fig. 6G). The influence of overexpression of RUNX3 on the expression of anti-apoptotic proteins in the presence of the MSC was determined by immunoblotting. Mcl-1 protein upregulation was observed in K562 cells grown with stromal cells. However, cells transfected with RUNX3 downregulated stroma-induced Mcl-1 levels in K562 cells (Fig. 6G).

Discussion

In this study, we examined the involvement of RUNX3 in As_2O_3-induced cellular apoptosis using the APL-derived, NB4 cell line and the CML-derived, K562 cell line. As_2O_3-induced expression of RUNX3 and nuclear localization of RUNX3 were both observed in NB4 and K562 cells. The transcriptional activation of RUNX3 following treatment with As_2O_3 was confirmed by the upregulation of p21, a target gene for RUNX3. It is now known that the generation of ROS is one of the major mechanisms through which As_2O_3 affects neoplastic cells. Treatment with NAC, a scavenger of ROS, resulted in the inhibition of As_2O_3-induced expression of RUNX3. Furthermore, knockdown of endogenous RUNX3 by shRNA blocked As_2O_3-induced apoptosis and cell cycle arrest in the K562 cell lines. Our data strongly suggest that RUNX3 may be a key molecule in a series of cellular responses induced by As_2O_3 treatment during leukemia therapy.

In this study, we provide evidence that a cell-contact mediated interaction between MSC and leukemia cells effectively protects leukemia cells from As_2O_3-induced cell death. In agreement with earlier results, we found that the leukemia-stroma interaction and the consequences that this interaction has on tumor survival following exposure to As_2O_3, involve CXCR4/CXCL12 signaling. However, the precise mechanism by which CXCR4/CXCL12 signaling guard leukemia cells from As_2O_3-induced apoptosis was unclear. In this study, we identified RUNX3 as a key transcription factor involved in the protection of leukemia cells through an interaction with MSC in As_2O_3-treated cell lines. We show at the protein level that the presence of CXCL12 or MSC the upregulation of RUNX3 that occurs during treatment of cells with As_2O_3. A CXCR4 antagonist, AMD3100, which blocks CXCL12/CXCR4 signaling, could efficiently rescue the expression of RUNX3. Regulation of RUNX3 expression appears to be the effect of CXCL12/CXCR4 signaling in K562 cells. This finding suggests that downregulation of RUNX3 expression is involved in the development of drug-resistance

signals derived from CML-MSC interactions. Taken together with our observation that active RUNX3 restores sensitivity of chronic myeloid leukemia cells to As_2O_3, MSC-induced drug-resistance in leukemia cells may be overcome by forced activation of RUNX3 and subsequent inhibition of Mcl-1.

Mcl-1 is an early response gene that functions as a regulator of cell viability (38). Mcl-1 can undergo rapid upregulation, as well as downregulation (39), which allows Mcl-1 to provide an acute protective function from apoptosis induced by various factors, including DNA damage (40), growth factor withdrawal (41,42) and treatment with cytotoxic agents (43). Western blot analysis suggested that Mcl-1 expression decreased in K562/RUNX3 and increased in K562/siRUNX3 compared with respective control cells. However, this result did not necessarily mean that RUNX3 was a transcriptional repressor of Mcl-1. Further study is needed to clarify the regulatory effects of RUNX3 on Mcl-1 expression. Mcl-1 protein upregulation was observed in K562 cells grown in the presence of stromal cells. The overexpression of RUNX3 downregulated endogenous as well as stroma-induced Mcl-1 levels in K562 cells. Those results suggest the induction of RUNX3 is associated with the expression of RUNX3 and bone marrow stromal cells may support K562 cells via induction of Mcl-1.

In summary, we report that RUNX3 plays a critical role in As_2O_3-induced apoptosis and CXCR4/CXCL12 signaling involved in the leukemia-stroma interaction. CXCR4/CXCL12 signaling downregulates the expression of the transcription factor RUNX3. Reduced levels of RUNX3 in turn compromise the apoptosis induced by As_2O_3. The overexpression of RUNX3 can effectively antagonize survival and drug-resistance signals derived from CML-MSC interactions.

References

1. Ding W, Knox TR, Tschumper RC, Wu W, Schwager SM, Boysen JC, Jelinek DF and Kay NE: Platelet-derived growth factor (PDGF)-PDGF receptor interaction activates bone marrow-derived mesenchymal stromal cells derived from chronic lymphocytic leukemia: implications for an angiogenic switch. Blood 116: 2984-2993, 2010.
2. Li W, Zhou Y, Yang J, Zhang X, Zhang H, Zhang T, Zhao S, Zheng P, Huo J and Wu H: Gastric cancer-derived mesenchymal stem cells prompt gastric cancer progression through secretion of interleukin-8. J Exp Clin Cancer Res 34: 52, 2015.
3. Arai F, Hirao A, Ohmura M, Sato H, Matsuoka S, Takubo K, Ito K, Koh GY and Suda T: Tie2/angiopoietin-1 signaling regulates hematopoietic stem cell quiescence in the bone marrow niche. Cell 118: 149-161, 2004.
4. Huang F, Wang M, Yang T, Cai J, Zhang Q, Sun Z, Wu X, Zhang X, Zhu W, Qian H, *et al*: Gastric cancer-derived MSC-secreted PDGF-DD promotes gastric cancer progression. J Cancer Res Clin Oncol 140: 1835-1848, 2014.
5. Vianello F, Villanova F, Tisato V, Lymperi S, Ho KK, Gomes AR, Marin D, Bonnet D, Apperley J, Lam EW, *et al*: Bone marrow mesenchymal stromal cells non-selectively protect chronic myeloid leukemia cells from imatinib-induced apoptosis via the CXCR4/CXCL12 axis. Haematologica 95: 1081-1089, 2010.
6. Sison EA and Brown P: The bone marrow microenvironment and leukemia: Biology and therapeutic targeting. Expert Rev Hematol 4: 271-283, 2011.
7. O'Hayre M, Salanga CL, Kipps TJ, Messmer D, Dorrestein PC and Handel TM: Elucidating the CXCL12/CXCR4 signaling network in chronic lymphocytic leukemia through phosphoproteomics analysis. PLoS One 5: e11716, 2010.
8. Li X, Guo H, Duan H, Yang Y, Meng J, Liu J, Wang C and Xu H: Improving chemotherapeutic efficiency in acute myeloid leukemia treatments by chemically synthesized peptide interfering with CXCR4/CXCL12 axis. Sci Rep 5: 16228, 2015.
9. Han TT, Fan L, Li JY and Xu W: Role of chemokines and their receptors in chronic lymphocytic leukemia: Function in microenvironment and targeted therapy. Cancer Biol Ther 15: 3-9, 2014.
10. Möhle R, Failenschmid C, Bautz F and Kanz L: Overexpression of the chemokine receptor CXCR4 in B cell chronic lymphocytic leukemia is associated with increased functional response to stromal cell-derived factor-1 (SDF-1). Leukemia 13: 1954-1959, 1999.
11. de Lourdes Perim A, Amarante MK, Guembarovski RL, de Oliveira CE and Watanabe MA: CXCL12/CXCR4 axis in the pathogenesis of acute lymphoblastic leukemia (ALL): A possible therapeutic target. Cell Mol Life Sci 72: 1715-1723, 2015.
12. Alsayed Y, Ngo H, Runnels J, Leleu X, Singha UK, Pitsillides CM, Spencer JA, Kimlinger T, Ghobrial JM, Jia X, *et al*: Mechanisms of regulation of CXCR4/SDF-1 (CXCL12)-dependent migration and homing in multiple myeloma. Blood 109: 2708-2717, 2007.
13. Nervi B, Ramirez P, Rettig MP, Uy GL, Holt MS, Ritchey JK, Prior JL, Piwnica-Worms D, Bridger G, Ley TJ, *et al*: Chemosensitization of acute myeloid leukemia (AML) following mobilization by the CXCR4 antagonist AMD3100. Blood 113: 6206-6214, 2009.
14. Sison EA, Magoon D, Li L, Annesley CE, Rau RE, Small D and Brown P: Plerixafor as a chemosensitizing agent in pediatric acute lymphoblastic leukemia: Efficacy and potential mechanisms of resistance to CXCR4 inhibition. Oncotarget 5: 8947-8958, 2014.
15. Shen ZH, Zeng DF, Ma YY, Zhang X, Zhang C and Kong PY: Are there any new insights for G-CSF and/or AMD3100 in chemotherapy of haematological malignants? Med Oncol 32: 262, 2015.
16. Kashyap MK, Kumar D, Jones H, Amaya-Chanaga CI, Choi MY, Melo-Cardenas J, Ale-Ali A, Kuhne MR, Sabbatini P, Cohen LJ, *et al*: Ulocuplumab (BMS-936564/MDX1338): A fully human anti-CXCR4 antibody induces cell death in chronic lymphocytic leukemia mediated through a reactive oxygen species-dependent pathway. Oncotarget 7: 2809-2822, 2016.
17. Niedermeier M, Hennessy BT, Knight ZA, Henneberg M, Hu J, Kurtova AV, Wierda WG, Keating MJ, Shokat KM and Burger JA: Isoform-selective phosphoinositide 3'-kinase inhibitors inhibit CXCR4 signaling and overcome stromal cell-mediated drug resistance in chronic lymphocytic leukemia: A novel therapeutic approach. Blood 113: 5549-5557, 2009.
18. Liu CC, Wang H, Wang WD, Zhu MY, Geng QR and Lu Y: Consolidation therapy of arsenic trioxide alternated with chemotherapy achieves remarkable efficacy in newly diagnosed acute promyelocytic leukemia. Onco Targets Ther 8: 3297-3303, 2015.
19. Soignet SL, Frankel SR, Douer D, Tallman MS, Kantarjian H, Calleja E, Stone RM, Kalaycio M, Scheinberg DA, Steinherz P, *et al*: United States multicenter study of arsenic trioxide in relapsed acute promyelocytic leukemia. J Clin Oncol 19: 3852-3860, 2001.
20. Shen Y, Shen ZX, Yan H, Chen J, Zeng XY, Li JM, Li XS, Wu W, Xiong SM, Zhao WL, *et al*: Studies on the clinical efficacy and pharmacokinetics of low-dose arsenic trioxide in the treatment of relapsed acute promyelocytic leukemia: A comparison with conventional dosage. Leukemia 15: 735-741, 2001.
21. Chendamarai E, Ganesan S, Alex AA, Kamath V, Nair SC, Nellickal AJ, Janet NB, Srivastava V, Lakshmi KM, Viswabandya A, *et al*: Comparison of newly diagnosed and relapsed patients with acute promyelocytic leukemia treated with arsenic trioxide: Insight into mechanisms of resistance. PLoS One 10: e0121912, 2015.
22. Lengfelder E, Lo-Coco F, Ades L, Montesinos P, Grimwade D, Kishore B, Ramadan SM, Pagoni M, Breccia M, Huerta AJ, *et al*; European LeukemiaNet: Arsenic trioxide-based therapy of relapsed acute promyelocytic leukemia: Registry results from the European Leukemia Net. Leukemia 29: 1084-1091, 2015.
23. Salmon JM, Bots M, Vidacs E, Stanley KL, Atadja P, Zuber J and Johnstone RW: Combining the differentiating effect of panobinostat with the apoptotic effect of arsenic trioxide leads to significant survival benefit in a model of t(8;21) acute myeloid leukemia. Clin Epigenetics 7: 2, 2015.
24. Oancea C, Rüster B, Brill B, Roos J, Heinssmann M, Bug G, Mian AA, Guillen NA, Kornblau SM, Henschler R, *et al*: STAT activation status differentiates leukemogenic from non-leukemogenic stem cells in AML and is suppressed by arsenic in t(6;9)-positive AML. Genes Cancer 5: 378-392, 2014.
25. Evens AM, Tallman MS and Gartenhaus RB: The potential of arsenic trioxide in the treatment of malignant disease: Past, present, and future. Leuk Res 28: 891-900, 2004.

26. Chen GQ, Shi XG, Tang W, Xiong SM, Zhu J, Cai X, Han ZG, Ni JH, Shi GY, Jia PM, *et al*: Use of arsenic trioxide (As_2O_3) in the treatment of acute promyelocytic leukemia (APL): I. As_2O_3 exerts dose-dependent dual effects on APL cells. Blood 89: 3345-3353, 1997.
27. Lallemand-Breitenbach V, Zhu J, Chen Z and de Thé H: Curing APL through PML/RARA degradation by As_2O_3. Trends Mol Med 18: 36-42, 2012.
28. Cai X, Shen YL, Zhu Q, Jia PM, Yu Y, Zhou L, Huang Y, Zhang JW, Xiong SM, Chen SJ, *et al*: Arsenic trioxide-induced apoptosis and differentiation are associated respectively with mitochondrial transmembrane potential collapse and retinoic acid signaling pathways in acute promyelocytic leukemia. Leukemia 14: 262-270, 2000.
29. Guan L, Han B, Li Z, Hua F, Huang F, Wei W, Yang Y and Xu C: Sodium selenite induces apoptosis by ROS-mediated endoplasmic reticulum stress and mitochondrial dysfunction in human acute promyelocytic leukemia NB4 cells. Apoptosis 14: 218-225, 2009.
30. Menheniott TR, Judd LM and Giraud AS: RUNX3 methylation and anti-tumor immunity. Oncoscience 2: 789-790, 2015.
31. Ito K, Liu Q, Salto-Tellez M, Yano T, Tada K, Ida H, Huang C, Shah N, Inoue M, Rajnakova A, *et al*: RUNX3, a novel tumor suppressor, is frequently inactivated in gastric cancer by protein mislocalization. Cancer Res 65: 7743-7750, 2005.
32. Yano T, Ito K, Fukamachi H, Chi XZ, Wee HJ, Inoue K, Ida H, Bouillet P, Strasser A, Bae SC, *et al*: The RUNX3 tumor suppressor upregulates Bim in gastric epithelial cells undergoing transforming growth factor beta-induced apoptosis. Mol Cell Biol 26: 4474-4488, 2006.
33. Chi XZ, Yang JO, Lee KY, Ito K, Sakakura C, Li QL, Kim HR, Cha EJ, Lee YH, Kaneda A, *et al*: RUNX3 suppresses gastric epithelial cell growth by inducing p21(WAF1/Cip1) expression in cooperation with transforming growth factor {beta}-activated SMAD. Mol Cell Biol 25: 8097-8107, 2005.
34. Ito K, Lim AC, Salto-Tellez M, Motoda L, Osato M, Chuang LS, Lee CW, Voon DC, Koo JK, Wang H, *et al*: RUNX3 attenuates β-catenin/T cell factors in intestinal tumorigenesis. Cancer Cell 14: 226-237, 2008.
35. Pande S, Ali SA, Dowdy C, Zaidi SK, Ito K, Ito Y, Montecino MA, Lian JB, Stein JL, van Wijnen AJ, *et al*: Subnuclear targeting of the Runx3 tumor suppressor and its epigenetic association with mitotic chromosomes. J Cell Physiol 218: 473-479, 2009.
36. Okorokov AL, Rubbi CP, Metcalfe S and Milner J: The interaction of p53 with the nuclear matrix is mediated by F-actin and modulated by DNA damage. Oncogene 21: 356-367, 2002.
37. Bae SC, Takahashi E, Zhang YW, Ogawa E, Shigesada K, Namba Y, Satake M and Ito Y: Cloning, mapping and expression of PEBP2 alpha C, a third gene encoding the mammalian Runt domain. Gene 159: 245-248, 1995.
38. Beekman AM and Howell LA: Small-molecule and peptide inhibitors of the pro-survival protein Mcl-1. Chem Med Chem 11: 802-813, 2016.
39. Belmar J and Fesik SW: Small molecule Mcl-1 inhibitors for the treatment of cancer. Pharmacol Ther 145: 76-84, 2015.
40. Cuconati A, Mukherjee C, Perez D and White E: DNA damage response and MCL-1 destruction initiate apoptosis in adenovirus-infected cells. Genes Dev 17: 2922-2932, 2003.
41. Bose P and Grant S: Mcl-1 as a Therapeutic Target in Acute Myelogenous Leukemia (AML). Leuk Res Rep 2: 12-14, 2013.
42. Lee WS, Park YL, Kim N, Oh HH, Son DJ, Kim MY, Oak CY, Chung CY, Park HC, Kim JS, *et al*: Myeloid cell leukemia-1 is associated with tumor progression by inhibiting apoptosis and enhancing angiogenesis in colorectal cancer. Am J Cancer Res 5: 101-113, 2014.
43. Lee JS, Tang SS, Ortiz V, Vo TT and Fruman DA: MCL-1-independent mechanisms of synergy between dual PI3K/mTOR and BCL-2 inhibition in diffuse large B cell lymphoma. Oncotarget 6: 35202-35217, 2015.